Examining nuclear effects in neutrino interactions with transverse kinematic imbalance

Luke Pickering[1]

[1]*Imperial College London*

E-mail: luke.pickering08@imperial.ac.uk

We present a Monte Carlo truth study examining nuclear effects in charged-current neutrino interactions using observables constructed in the transverse plane. Three distributions are introduced that show very weak dependence on neutrino flux and its associated uncertainty. Measurements comparing these distributions between quasi-elastic-like and single charged pion final states will provide new constraints of nuclear effects. It is suggested that the on-axis position in the NuMI beam provides the correct flux to take advantage of this reduced energy dependence in measuring nuclear effect-generated transverse imbalances.

KEYWORDS: neutrino-nucleus interaction, neutrino energy dependence, nuclear effects, transverse plane

1. Introduction

Correctly reconstructing the energy of a neutrino interaction is an important part of both neutrino oscillation and neutrino scattering physics. Using nuclear targets, as opposed to free nucleon targets, obfuscates the neutrino interaction and imparts significant uncertainties and model dependencies onto the reconstructed neutrino energy. Current neutrino beams are wide-band and the spread in event-by-event neutrino energy is significant, thereby making the impact of nuclear effects difficult to isolate. Understanding the hadronic system is key for investigations of nuclear effects; it holds all available information about the type of interaction that occurred.

This talk presents a Monte Carlo truth study into the use of variables defined in the plane transverse to the incoming neutrino. In the absence of nuclear effects, the transverse momentum in the final state should be identically balanced. Therefore, nuclear effects that affect the kinematics of final state particles can be seen as deviations from finely balanced systems. For more details the reader is directed to [1].

This study mainly examines predictions from the NuWro generator [2]. However, NEUT [3], GENIE [4], and GiBUU [5] have also been investigated and the procedures used are fully generator-independent.

2. Energy Transfer and Hadronic System Energy in QE and RES Interactions

For quasi-elastic (QE [7]) and resonant pion production (RES [8]) neutrino interactions the phase space for four momentum transfer, Q^2, is bounded. At larger four momentum transfer, the mediating particle scatters off quarks and results in so called deep inelastic scatters. Fig. 1 shows the NuWro predicted event rate for QE and RES interactions, as a function of Q^2 for a number of different neutrino fluxes. For neutrino energies $\lesssim 2$ GeV, the Q^2 shape changes significantly with increasing neutrino energy. However, the shape change between 3 GeV and 6 GeV is minimal. For QE and RES interactions at these energies, the models predict that almost all of the possible Q^2 phase space for

that interaction type is kinematically accessible. Predicted event rates for interactions in a real beam with a wide spectral shape and peaked at sufficiently high energy, such as the NuMI on-axis beam [6], also exhibit the same Q^2 shape.
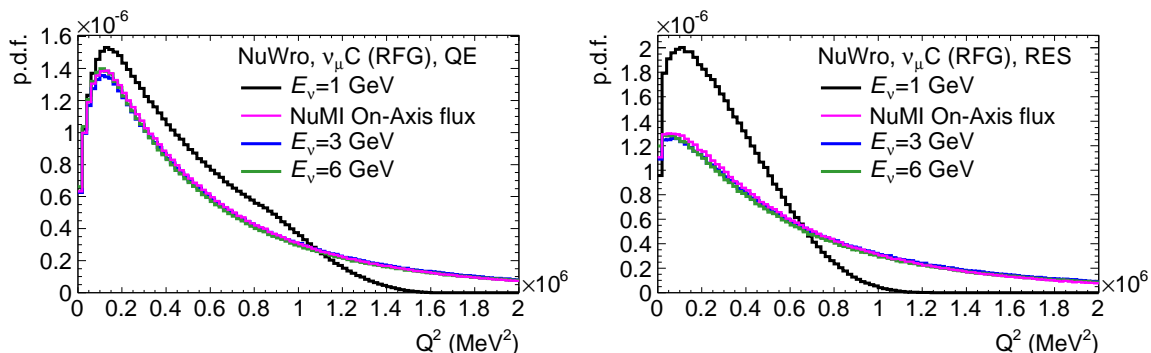

Fig. 1. Four momentum transfer for QE (Llewellyn Smith [7]) and RES (Rein Sehgal [8]) interactions as predicted by NuWro. The Q^2 shape is asymptotically independent of the neutrino energy above some threshold, leading to decoupling of the neutrino energy and the energy of the final state hadronic system. The NuMI on-axis beam is sufficiently high energy to cause this decoupling in both the QE and RES channels.

In a neutrino interaction where a single hadronic particle, with invariant hadronic mass W, is excited from an initial state nucleon, N, the energy transfer, ω, can be written as

$$\omega = \frac{Q^2 + W^2 - m_N^2}{2\sqrt{m_N^2 + p_N^2}},$$

where m_N and p_N are the mass and three momentum of the initial state nucleon. For QE interactions, $\nu_\mu + n \rightarrow \mu + p$, W is the proton mass. For RES interactions, hadronic mass cuts that isolate single pion production via a delta resonance are frequently used, *e.g.* in MINERvA charged current single pion production [9]. This results in a hadronic mass distributed about 1.2 GeV. The initial state nucleon momentum distribution is separate from the neutrino interaction. The only remaining unknown is Q^2. As discussed, above some threshold energy, Q^2 is largely independent of the neutrino energy. Therefore, in an appropriate neutrino beam, the event-by-event energy transfer to the hadronic system should be largely decoupled from the neutrino energy. The on-axis position in the NuMI beam has a peak energy high enough to cause such decoupling for QE and for RES events. The following discussions focus on NuWro predicted event rate shapes for a carbon target exposed to the NuMI on-axis muon neutrino flux.

3. Transverse Variables in QE Interactions

3.1 Definition

Fig. 2 shows the schematic definitions of three variables defined in the plane transverse to the incoming neutrino, δp_T, $\delta\alpha_T$, and $\delta\phi_T$.

These three variables are defined as:

$$\delta\vec{p}_T = \vec{p}_T^{\ell} + \vec{p}_T^{p},$$
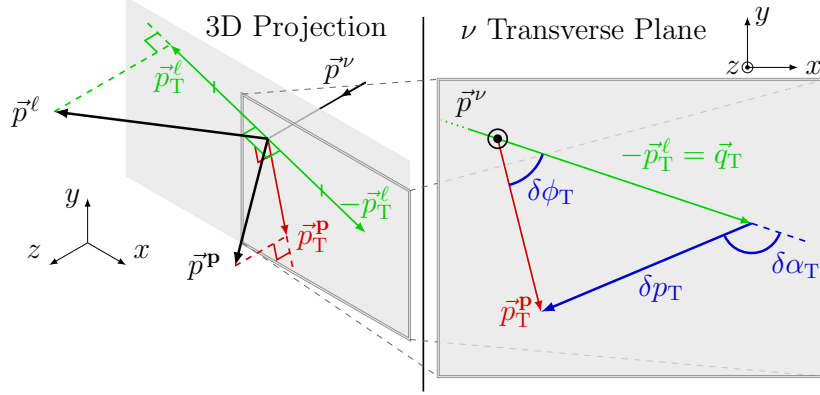
2

Fig. 2. A schematic definition of three transverse variables, δp_T, $\delta \alpha_T$, and $\delta \phi_T$, in a QE muon neutrino interaction.

$$\delta \phi_T = \arccos \frac{-\vec{p}_T^{\ell} \cdot \vec{p}_T^{N}}{p_T^{\ell} p_T^{N}}, \text{ and}$$

$$\delta \alpha_T = \arccos \frac{-\vec{p}_T^{\ell} \cdot \delta \vec{p}_T}{p_T^{\ell} \delta p_T}.$$

δp_T is the overall three momentum imbalance in the transverse plane. In the absence of nuclear effects—and detector effects—δp_T should be described by a Dirac delta function at $\delta p_T = 0$. The transverse momentum imbalance has been investigated in neutrino scattering previously. The Big European Bubble Chamber examined transverse momentum imbalance in deuterium exposed to wide band neutrino beams at the CERN SPS [10]. Their data set is significantly dominated by deep inelastic scattering events due to the beam energy. NOMAD used transverse kinematic imbalance as a selection variable for QE events, also in a higher energy beam than used by current neutrino experiments (which require $O(\text{GeV})$ beams for use in neutrino oscillation physics) [11].

$\delta \phi_T$ describes the angular difference between the observed final state and the case where the final state particles are back-to-back in the transverse plane. A highly balanced system is characterised by $\delta \phi_T = 0$. $\delta \phi_T$ has been used in QE event classifiers at NOMAD and INGRID [11,12]. The MINERvA collaboration measured the *coplanarity angle*, $\varphi = \pi - \delta \phi_T$, in their 'CC with no pions in the final state' event selection and find their data to largely agree with a GENIE simulation [13].

$\delta \alpha_T$ can be used to classify a process as having an 'accelerating' or 'decelerating' effect on the hadronic system. For $\delta \alpha_T < 90°$ the proton transverse momentum appears larger than expected from the observed muon transverse momentum—an apparently accelerating effect–and it appears less than expected for $\delta \alpha_T > 90°$. $\delta \alpha_T$ was proposed and investigated for the first time in a recent truth study [1].

Monte Carlo predictions for these three variables are presented in the following sections along with discussions of features predicted by individual nuclear effects.

3.2 Energy dependence of the transverse variables

δp_T is directly generated by nuclear effects. The direction of this transverse momentum imbalance with respect to an axis defined by the charged lepton defines $\delta \alpha_T$. Fig. 3 shows how, over an order of magnitude of beam energies, the change in the shape of δp_T and $\delta \alpha_T$ is minimal. This is not the case for charged lepton final state kinematics alone. Such energy independence is desirable when attempting to isolate the effects of using a nuclear target from the effects of a wide-band neutrino beam.

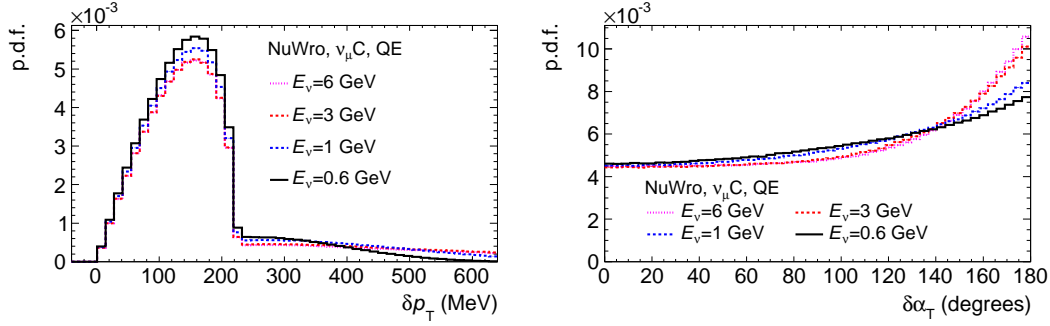However, the shape of $\delta \phi_T$ is more strongly influenced by the neutrino energy. This is because

Fig. 3. Both δp_T , (*left*), and $\delta\alpha_T$, (*right*), exhibit less neutrino energy dependence than final state lepton kinematics.

of the trigonometric dependence on the magnitude of the muon transverse momentum. Fig. 4 shows how for a given δp_T and $\delta\alpha_T$, the resulting $\delta\phi_T$ depends more strongly on the kinematics of the neutrino interaction rather than just on the largely decoupled hadronic system. When naively examining $\delta\phi_T$, flux uncertainties are still more conflated with FSI uncertainties. One way to account for this dependence is to perform a double differential measurement of $\frac{d^2\sigma}{d\delta p_T dp_T^\ell}$.
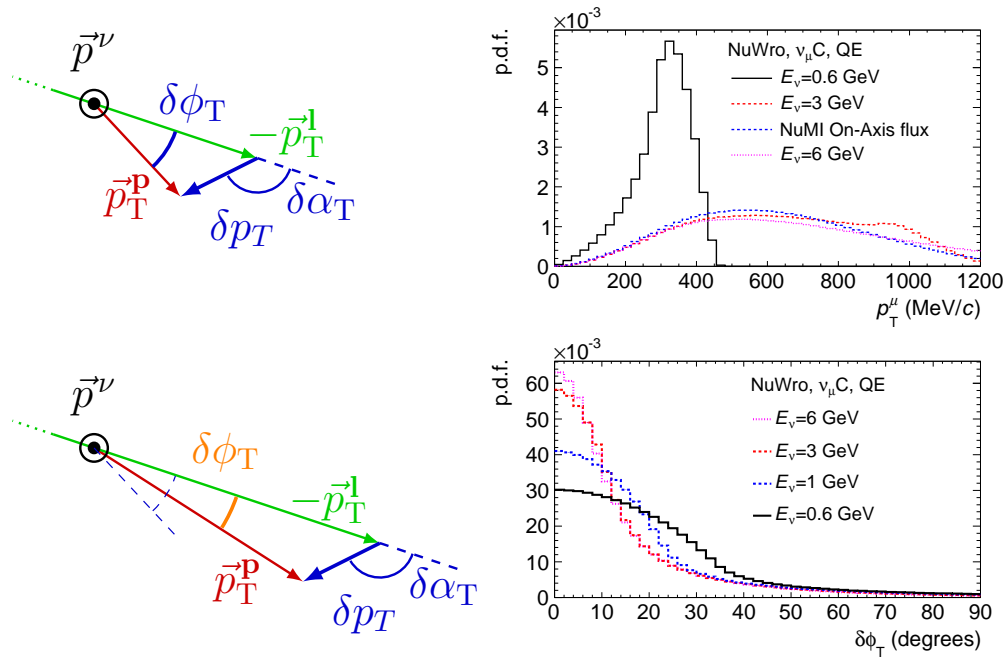

Fig. 4. (*left*): For a given δp_T and $\delta\alpha_T$, which are generated by distinct nuclear effects independent of the charged lepton kinematics, the observed $\delta\phi_T$ depends on the magnitude of p_T^ℓ. (*top right*): The p_T^ℓ distribution varies strongly as a function of neutrino energy. (*below left*): For more energetic neutrinos, $\delta\phi_T$ has a tighter peak due to the distribution of p_T^ℓ, however, FSIs result in a broader peak.
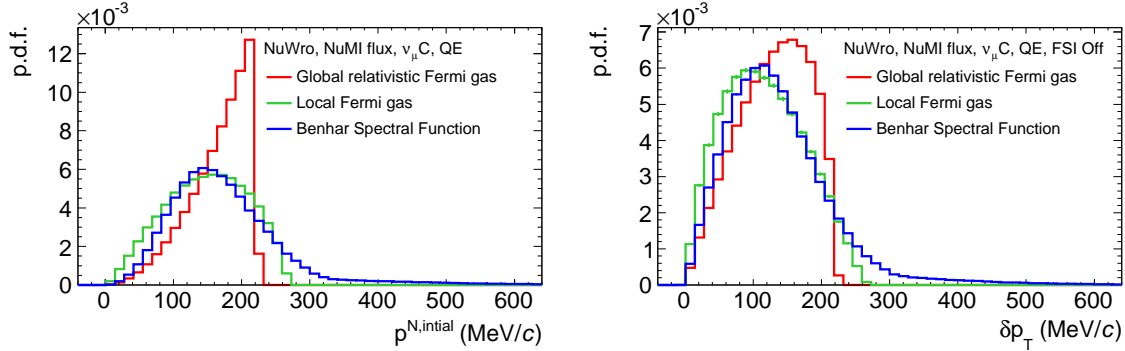
Fig. 5. (*left*) The magnitude of the nucleon momentum distribution for three widely used nuclear models (global relativistic Fermi gas (RFG), local Fermi gas (LFG), and Benhar spectral function (SF) [14]). (*right*) The apparent transverse momentum resulting from the nucleon Fermi motion, for QE interactions.

3.3 Transverse Variables as Probes of Nuclear Effects

3.3.1 Fermi motion

When neutrinos scatter from free nucleons at rest, it is expected that the transverse momentum of the final state particles identically balance: $\delta p_T = 0, \delta\phi_T = 0, \delta\alpha_T$ is undefined. In a nuclear environment the nucleons are undergoing random Fermi motion which imparts an unknowable event-by-event boost to the interacting system. This boost introduces a characteristic shape to each of the three distributions.

In the absence of any Final State Interactions (FSIs) the apparent momentum imbalance in the lab frame is generated purely by the Fermi motion of the struck nucleon. δp_T is therefore distributed according to the transverse component of the Fermi motion. Fig. 5 shows how differences in the nuclear model are reflected in lab-frame δp_T distributions.
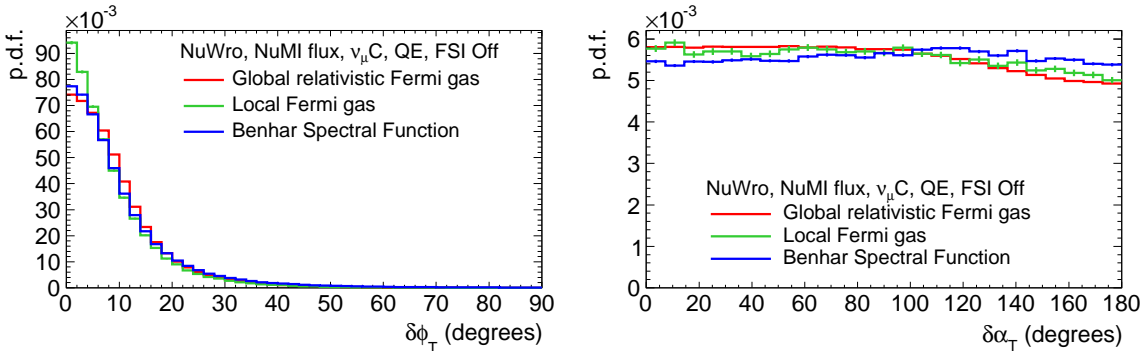

Fig. 6. The $\delta\phi_T$ (*left*), and $\delta\alpha_T$ (*right*), predictions for three nuclear models in the absence of FSIs.

Fig. 6 shows the 'FSI-off' predictions for $\delta\phi_T$ and $\delta\alpha_T$. $\delta\phi_T$ gains some width as a result of the unknown boost; the distribution is strongly peaked around $\delta\phi_T = 0$. $\delta\alpha_T$ can be defined for any transverse momentum imbalance $\delta p_T \neq 0$. However, we expect the Fermi motion to be isotropic resulting a flat distribution for the apparent acceleration or deceleration of the proton.
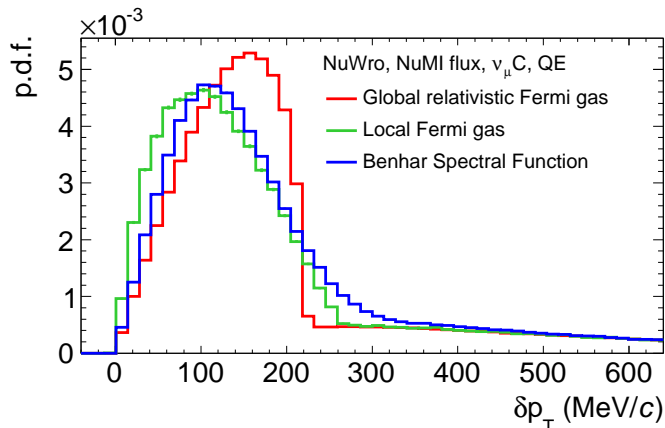
Fig. 7. The fully simulated transverse momentum imbalance for three nuclear models. Low δp_T is dominated by the transverse projection of the nucleon momentum distribution, as in Fig. 5. At larger transverse momemtum imbalances, the δp_T distribution becomes largely independent of the initial state because of FSI smearing.

3.3.2 Final State Interactions

FSIs can refer to any re-scattering of the final hadronic system as it leaves the nucleus. This includes: elastic and inelastic re-scatters, absorption, charge exchange, or spectator nucleon knock-out. These processes all act to obscure the hadronic system 'memory' of the interaction.

Fig. 7 shows the δp_T distributions for the three nuclear models. For δp_T less than the Fermi momentum, k_f, the distribution is almost entirely governed by the Fermi motion and for $\delta p_T \gtrsim 2k_f$ are independent of the initial state and instead indicative of the FSI model. The $\delta\phi_T$ distribution continues to broaden when FSI effects are enabled in the simulation.

Herein the global relativistic Fermi gas (RFG) model will be used as the nuclear model for the sake of simplicity. The other nuclear models have been investigated and the results are qualitatively similar. The RFG model is very simple, and not the most realistic model. When analyzing measured data, the most appropriate nuclear model should be used.

It might be naively expected that FSI processes generally transfer energy from the vertex-exiting hadronic system to the nuclear environment. The simulated distributions agree with these expectations, showing that FSIs cause a pile-up of events at $\delta\alpha_T \sim 180°$—characteristic of an apparently decelerated hadronic system.

Fig. 8 shows how $\delta\alpha_T$ varies with p_T^ℓ with and without FSIs enabled in the simulation. The transverse momentum of the charged lepton is correlated with the pre-FSI transverse momentum of the final state hadron, up to k_f. Measuring transverse kinematic imbalance as a function of the lepton momentum may allow new insight into FSI processes. Such a measurement would be complementary to the thin target hadron scattering data typically used to tune FSI simulations, e.g. [15, §2.5]. It may be the case that intra- and extra-nuclear forces are considerably different, making an in-channel FSI constraint invaluable.

3.3.3 Pauli Blocking

Pauli blocking reduces the interaction cross section by limiting the phase space for final state nucleon production. Values of Q^2 which would result in a final state nucleon in a quantum mechanical state that is already 'filled', are disallowed. For the global RFG nuclear model this corresponds to $p^p \leq k_f$. Comparison between Fig. 8 (*left*) and Fig. 9 (*below left*) shows that Pauli blocking causes a suppression at $\delta\alpha_T \sim 180°$ for $p_T^\mu \lesssim k_f$. This region corresponds to events where a small three
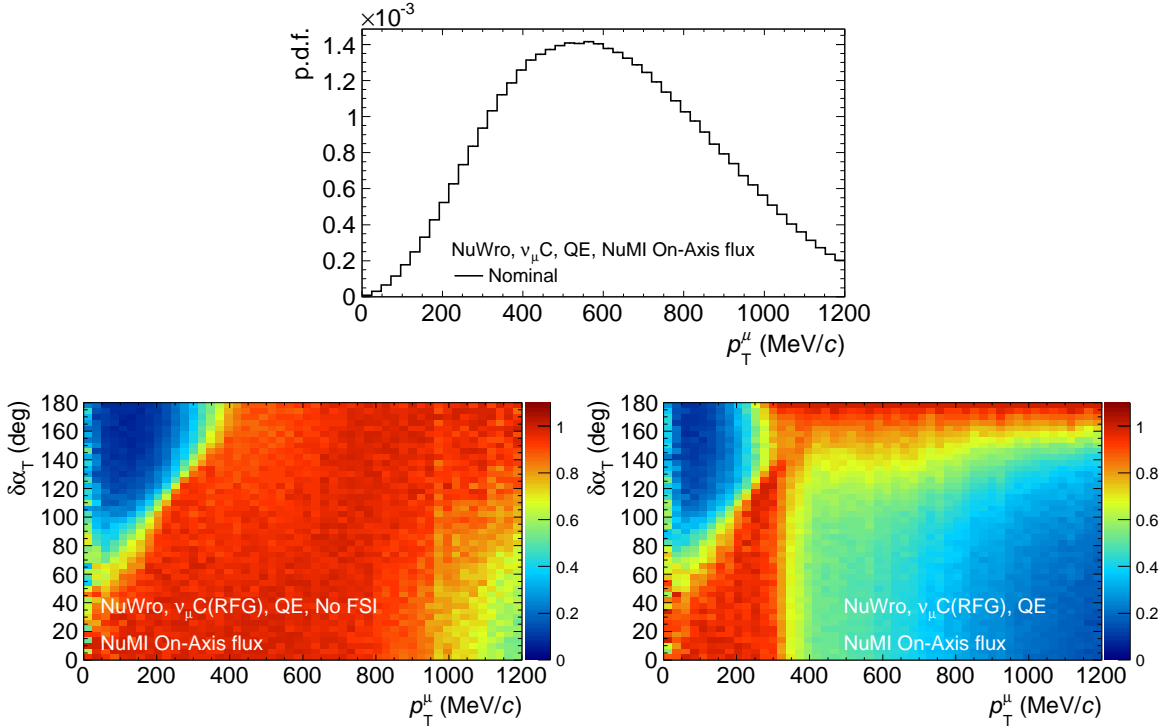
Fig. 8. (*top*) The NuWro predicted p_T^ℓ event rate for QE events on carbon in the NuMi On-Axis beam. p_T^ℓ slice-normalised $\delta\alpha_T$ v.s p_T^ℓ distributions, without (*bottom left*), and with (*bottom right*), FSIs enabled. FSIs cause the final state hadronic system to lose momentum as it leaves the nucleus, resulting in more events with large $\delta\alpha_T$.

momentum transfer acts against the initial state nucleon's Fermi motion, resulting in a final state hadron with momentum below the Fermi surface—causing Pauli blocking. Pauli blocking is also implemented in other nuclear models and the predicted effect is qualitatively similar.

4. Transverse Variables in Resonant Charged Pion Production

So far all discussions have been framed in the context of QE events. However, the resonance production system is expected to be similarly balanced for free nucleon targets. Fig. 10 shows the definitions of the transverse imbalances for a $1\mu + 1p + 1\pi$ final states. The impact of nuclear effects on transverse imbalance in RES interactions may differ from QE. FSIs of both protons and charged pions will be evident in these distributions. Pauli blocking will reduce the phase space for the resonance decay, but not limit the four momentum transfer phase space of the delta resonance production.

For the QE case it is not simple to examine transverse imbalance in an anti-neutrino beam: the final state hadron is neutral, so accurate detection becomes problematic. However, possible resonance production interactions, such as $\bar\nu_\ell + p \to \ell^+ + \Delta^0 \to \ell^+ p + \pi^-$, produces only charged final state hadrons. It is therefore possible to compare transverse imbalance across three channels: QE, Δ^{++}, and Δ^0, with three distinct final states. Fig. 11 shows the fully simulated transverse imbalance distributions for these three interaction channels.

5. Challenges

The transverse observable approach outlined aboves requires specific final states, whichy may differ from the original neutrino interaction. However, it provides a number of unique benefits. As
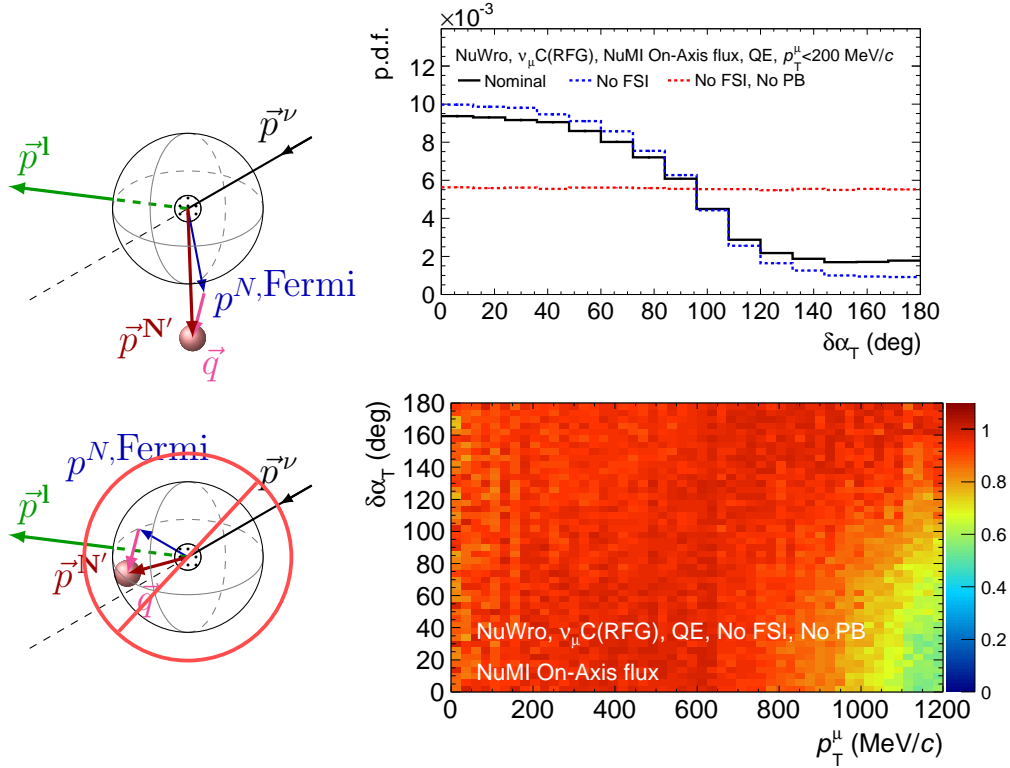
Fig. 9. (*left*): Pauli blocking (PB) suppresses events at low p_T^ℓ and high $\delta\alpha_\mathrm{T}$ because in this region a low three momentum transfer would act against the nucleon Fermi motion leaving it in a disallowed final state. (*top right*): The high $\delta\alpha_\mathrm{T}$ event suppression is due to Pauli blocking and acts against the effects of FSIs at low p_T^ℓ. (*below right*): p_T^ℓ slice-normalised event rate in $\delta\alpha_\mathrm{T}$ and p_T^ℓ. With Pauli blocking effects and FSIs removed from the simulation $\delta\alpha_\mathrm{T}$ is very flat in p_T^ℓ.
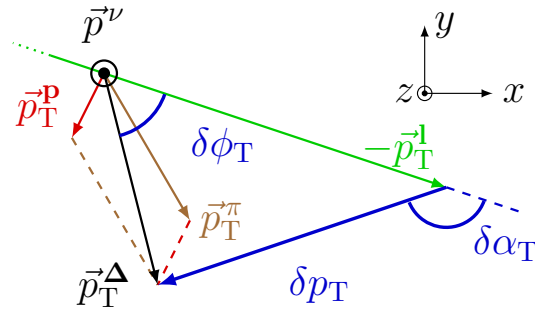

Fig. 10. A schematic definition of three transverse variables in a resonant single pion production interaction.

discussed, it is possible to make these measurements with a minimal degree of neutrino energy dependence. The distributions are not model dependent in their reconstruction, unlike Q^2 and ω that require assumptions on the neutrino-nucleus interaction vertex. Measuring transverse imbalance in neutrino scattering highlights the effects of FSIs on neutrino interactions, rather than inferring from the results of thin-target hadron scattering data. The distributions are constructed from leptonic and hadronic information, so will be naturally exclusive measurements. This means they will be a powerful test of the full predictions of interaction and FSI models.

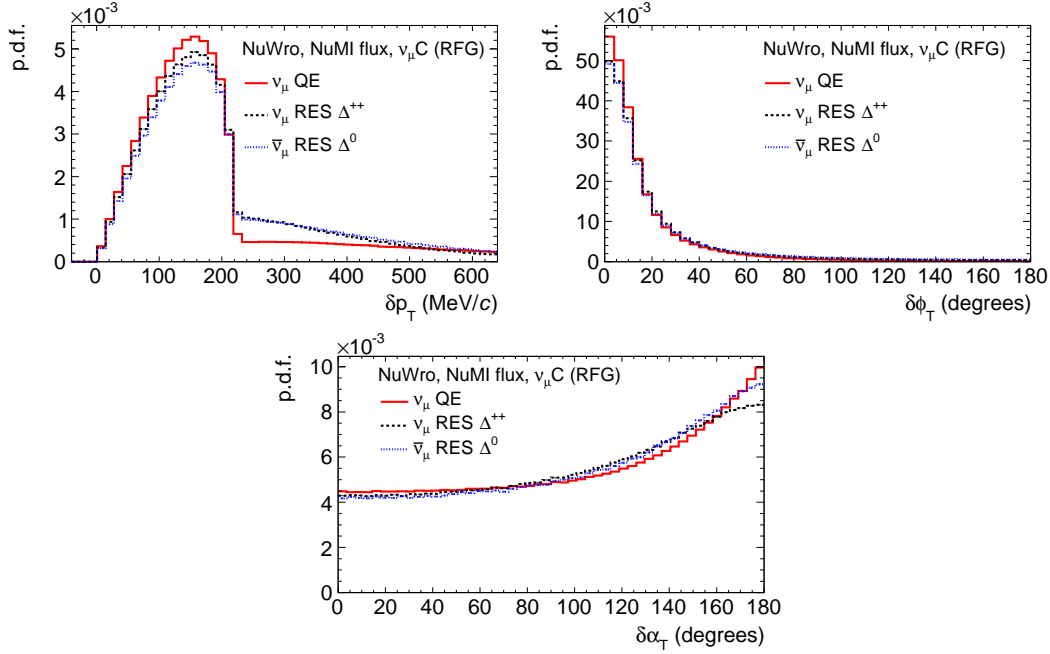Comparisons between nuclear effect-induced transverse imbalance in the three neutrino interac-

Fig. 11. The predicted transverse imbalance for QE, Δ^{++}, and Δ^0 resonances. The effect of charge pion FSI can be seen most apparently as an increased number of events in the FSI-dominated region of δp_T . Measurements of these distributions will act as direct probes of proton and proton + charged pion FSIs.

tion channels will give insight into intra-nuclear proton and charged pion interactions. This is one of a number of complementary approaches we think is important for tackling this highly convoluted problem.

6.   Summary

The hadronic portion of the final state is vital for identifying and understanding neutrino interactions. As discussed, nuclear effects obscure the primary neutrino interaction by modifying the observed final states. A number of the effects of using nuclear targets have been discussed in this talk and the impact on a set of transverse variables have been shown. Measurements of the distributions presented will provide a powerful way to gain insight into nuclear effects, with a reduced dependence on neutrino energy.

Acknowledgments

References

[1] X-G. Lu, *et al.*: arXiv:1512.05748 [nucl-th] (2015).

[2] Phys. Rev. C **86** 015505 (2012)

[3] Hayato, Acta Physica Polonica B **40**, 2477 (2009)

[4] C. Andreopoulos, *et al.*, Nucl. Instrum. Meth. **A614** 87-104 (2010)

[5] Phys. Rep. **512**, 1-124 (2012).

[6] See Appendix A.

[7] C.H. Llewellyn Smith, Phys. Rep. **3**, 261 (1972).

[8] D. Rein and L. M. Sehgal, Ann. Phys. (NY) **133**, 79 (1981)

[9] B. Eberly, *et al.*, arXiv:1406.6415v3 [hep-ex] (2015)

[10] Z. Phys. C - Particles and Fields **27**, 239-248 (1985)

[11] Eur.Phys.J. **C63**, 355-381 (2009)

[12] Phys. Rev. D. **91**, 112002 (2015).

[13] Phys. Rev. D **91**, 071301 (2015)

[14] O. Benhar, *et al.*, Phys. Rev. D **72**, 053005 (2005)

[15] C. Andreopoulos, *et al.*: arXiv:1510.05494 [hep-ph] (2015)
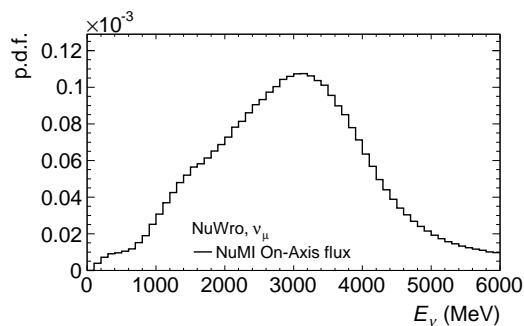
Appendix A: NuMI Flux

Fig. A·1.   The NuMI flux shape, as obtained from the NuWro source.

Appendix B: Code

During this work it was advantageous to examine the MC generator output in an as-generator-agnostic way as possible. To this end, code was written to allow conversion from the native GiBUU and NEUT outputs to the so-called `rootracker` output—both NuWro and GENIE already come with bundled software that can output in this format. Further more the `rootracker` event vectors were further processed into ROOT-based analysis files. All of the code is open source and available upon request. Discussions of designing a better event format than `rootracker` are very welcome.